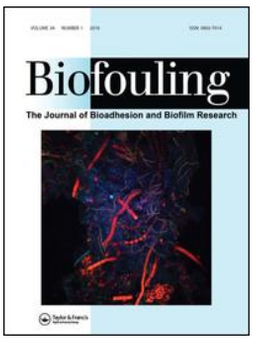

Taylor & Francis
Taylor & Francis Group

Biofouling
The Journal of Bioadhesion and Biofilm Research

ISSN: 0892-7014 (Print) 1029-2454 (Online) Journal homepage: http://www.tandfonline.com/loi/gbif20

Role of nutrient limitation in the competition between uropathogenic strains of Klebsiella pneumoniae and Escherichia coli in mixed biofilms

Guillermo E. Juarez & Estela M. Galván

To cite this article: Guillermo E. Juarez & Estela M. Galván (2018) Role of nutrient limitation in the competition between uropathogenic strains of Klebsiella pneumoniae and Escherichia coli in mixed biofilms, Biofouling, 34:3, 287-298, DOI: 10.1080/08927014.2018.1434876

To link to this article: https://doi.org/10.1080/08927014.2018.1434876

BIOFOULING, 2018
VOL. 34, NO. 3, 287–298
https://doi.org/10.1080/08927014.2018.1434876

Taylor & Francis
Taylor & Francis Group

Role of nutrient limitation in the competition between uropathogenic strains of *Klebsiella pneumoniae* and *Escherichia coli* in mixed biofilms

Guillermo E. Juarez[a,b] and Estela M. Galván[a,b,c]

[a]Laboratory of Bacterial Genetics, Fundacion Instituto Leloir-IIBBA (CONICET), Buenos Aires, Argentina; [b]Centro de Estudios Biomédicos, Biotecnológicos, Ambientales y Diagnóstico (CEBBAD), Universidad Maimónides, Buenos Aires, Argentina; [c]Carreras de Farmacia y Bioquímica, Facultad de Ciencias de la Salud, Universidad Maimónides, Buenos Aires, Argentina

ABSTRACT

Klebsiella pneumoniae and *Escherichia coli* form mixed species biofilms in catheter-associated urinary tract infections. Recently, a detrimental effect of *K. pneumoniae* over *E. coli* was observed in mixed species biofilms grown in an artificial urine medium. The mechanism behind this competitive interaction was studied. *K. pneumoniae* partially outcompeted *E. coli* in early-stage batch-fed biofilms, whereas both microorganisms co-exist at longer times (*K. pneumoniae*:*E. coli* ratio, 55:1), as shown by cell counts and confocal microscopy. *E. coli* cells were scattered along the *K. pneumoniae* biofilm. Biofilm supernatants did not appear to contain either antimicrobial or anti-biofilm activities against *E. coli*. Biofilms grown under continuous flow prevented interspecies competition. *K. pneumoniae* showed both increased siderophore production and better growth in iron-limited media compared to *E. coli*. In summary, these results indicate the importance of nutrient (particularly iron) competition in the modulation of the bacterial composition of mixed species biofilms formed by uropathogenic *K. pneumoniae* and *E. coli*.

ARTICLE HISTORY
Received 4 December 2017
Accepted 23 January 2018

KEYWORDS
Uropathogens; *Klebsiella pneumoniae*; *Escherichia coli*; mixed biofilms; interspecies competition; nutrient limitation

Introduction

The biofilm mode of growth is a basic survival strategy deployed by bacteria in a wide range of environmental, industrial and clinical settings (Flemming et al. 2016). The catheterized urinary tract provides ideal conditions for the development of biofilm populations. Consequently, catheter-associated urinary tract infections (CAUTIs) are among the most common nosocomial infectious diseases of humans, and significantly burden the healthcare system by increasing both morbidity and treatment costs (Chenoweth et al. 2014). Initial infections are usually caused by a single bacterial species, such as uropathogenic *Escherichia coli* or *Enterococcus faecalis* (Sabir et al. 2017). However, over time, a variety of organisms, including *Klebsiella pneumoniae*, *Pseudomonas aeruginosa*, *Proteus mirabilis* and *Morganella morganii* can colonize the urinary tract and form polymicrobial communities that are embedded in protective self-produced extracellular polymeric substances (Warren et al. 1982; Stickler 2008; Holá et al. 2010). Biofilm-associated infections are highly persistent because biofilms are much less susceptible to antimicrobials compared to planktonic cells (Hall-Stoodley et al. 2004).

Given the diversity of biofilms in nature, it is likely that interspecies interactions play important roles that impact the development, structure and function of these biofilms. Polymicrobial growth allows interspecies interactions that involve communication, usually *via* quorum sensing. These interactions can be of a cooperative (synergistic), competitive (antagonistic) or neutral nature (Tan et al. 2017). Synergistic interactions are based on promotion of biofilm formation by co-aggregation, metabolic cooperation (one species utilizes a metabolite produced by a neighboring species), and can also increase resistance to antibiotics or host immune responses compared to mono-species biofilms. On the other hand, antagonistic interactions are based on competition for nutrients and growth inhibition (Burmolle et al. 2006; Harriott and Noverr 2009).

Recently, a high prevalence of *K. pneumoniae* and *E. coli* co-isolates in catheter-associated polymicrobial bacteriuria was shown (Galván et al. 2016). Moreover, the *in vitro* ability of these strains to establish mixed biofilms was reported. However, the mechanisms behind the interactions between these two species in mixed biofilms are still unknown. *K. pneumoniae* and uropathogenic *E. coli* are Gram-negative bacteria present in the human

CONTACT Estela M. Galván galvan.estela@maimonides.edu
Supplemental material for this paper (Figures S1 and S2) are linked to the article DOI online https://doi.org/10.1080/08927014.2018.1434876.

fecal flora as innocuous commensal bacteria inhabiting the colon. Despite that, under certain conditions, such as in immunocompromised individuals or when the mucosae is damaged by a disease, trauma, or catheterization, both organisms can induce infections (Moreno et al. 2006; Foxman 2014). Bacterial fimbriae are important for biofilm formation on catheters; *K. pneumoniae* uses mainly type 3 fimbriae whereas *E. coli* utilizes type 1 fimbriae (Schroll et al. 2010; Reisner et al. 2014). Nitrogen, iron and amino acids are essential nutrients for the survival of uropathogens during CAUTI development (Alteri and Mobley 2015; Subashchandrabose and Mobley 2015). Since the host environment is limited in available iron, to be able to grow in human urine uropathogens utilize a variety of iron uptake strategies, including siderophore systems for iron (Fe^{3+}) scavenging (Barber and Elde 2015). In the context of the urinary tract, both *K. pneumoniae* and *E. coli* strains produce some or all of the following siderophores: enterobactin, salmochelin, aerobactin and yersiniabactin (Henderson et al. 2009; El Fertas-Aissani et al. 2013). In particular, *E. coli* mutants lacking the iron uptake receptor responsible for iron acquisition through yersiniabactin showed impaired biofilm formation in urine medium (Hancock et al. 2008).

Knowledge of interspecies interactions between uropathogens that develop multispecies biofilms on urinary catheters, particularly *K. pneumoniae* and *E. coli*, is limited. *E. coli* has been studied in mixed species biofilms with *P. aeruginosa* (Cerqueira et al. 2013) and with two non-pathogenic atypical species (*Delftia tsuruhatensis* and *Achromobacter xylosoxidans*) (Azevedo et al. 2014). The results indicated that cell numbers of *E. coli* decreased when co-cultured with *P. aeruginosa* while *P. aeruginosa* seemed to benefit in mixed species biofilms (Cerqueira et al. 2013). On the other hand, pre-colonization with *Delftia tsuruhatensis* and *Achromobacter xylosoxidans* appeared to promote *E. coli* adhesion to form mixed species biofilms (Azevedo et al. 2014). Additionally, it has been reported that co-infection of the urinary tract with *E. coli* and *P. mirabilis* enhanced bacterial colonization and persistence of both pathogens during urinary tract infection (UTI), which is consistent with the observed changes in nutritional requirements between *E. coli* and *P. mirabilis* during co-colonization (Alteri et al. 2015). Finally, *in vitro* analysis of mixed *K. pneumoniae*–*E. coli* biofilms grown on a siliconized surface in artificial urine medium (AUM) showed a detrimental effect of *K. pneumoniae* over *E. coli* (Galván et al. 2016).

The present study focused on the elucidation of the mechanisms involved in the competitive interactions observed between *K. pneumoniae* and *E. coli* in mixed species biofilms developed in AUM. The interactions between these two microorganisms were studied over the course of nine days by both colony forming unit (CFU) counts and confocal laser scanning microscopy. The presence of secreted antimicrobial or anti-biofilm compounds was evaluated by analyzing biofilm supernatants. Additionally, the role of nutrient limitation was studied by comparing batch-fed *vs* dynamic biofilms. The results obtained help to better understand the interactions between *K. pneumoniae* and *E. coli* in mixed biofilms in the context of the urinary tract.

Materials and methods

Bacterial strains and inoculum preparation

Klebsiella pneumoniae 01 (Kp01, Ap^R) and *Escherichia coli* 01 (Ec01, Rf^R) clinical strains were co-isolated from a urine sample of a patient undergoing long-term catheterization of the urinary tract and showing symptoms of CAUTI (Galván et al. 2016). Isolates were maintained in the laboratory as frozen stocks (at –80°C) in Luria-Bertani (LB) broth supplemented with 15% glycerol. Inocula for assays were prepared as follows. Strains were freshly streaked on LB-agar plates and grown overnight at 37°C. Subsequently, individual colonies were used to inoculate LB broth and were incubated overnight at 37°C and 200 rpm. Then, each inoculum was properly diluted in artificial urine medium (AUM) (Brooks and Keevil 1997) or LB broth in order to obtain a desired final cell density. For dual-species assays, equal volumes of each single-species inoculum in AUM were mixed.

Biofilm formation assays

Bacterial inocula in AUM (1×10^7 CFU ml^{-1}) were placed in 24-well culture plates (GBO Cellstar, Frickenhausen, Germany), 1 ml per well, or in 60 mm-diameter culture dishes (GBO Cellstar), 8 ml per dish. It is well known that hydrophobic surfaces, such as silicone and polystyrene, are favorable surfaces for biofilm formation. The inoculated wells were incubated for 3 h to allow adhesion to the polystyrene surface. For batch-fed biofilm cultures, AUM was replaced every 24 h, as already described (Galván et al. 2016). For continuous-flow biofilm cultures, a flow cell system was made by making holes in the culture dishes and delivering the growth medium through a tubing system *via* a peristaltic pump, at a flow rate of 37 ml h^{-1} without recirculation. This flow rate is within the range established as normal urinary output for an adult (measured in a 24-h volume) and has been previously used (Stickler and Morgan 2006). The plates and dishes were incubated at 37°C. At selected time points, aliquots of the AUM surrounding the biofilms (biofilm supernatants) were saved and biofilms were washed three-times with sterile 0.9% NaCl before they were mechanically disrupted from the surface by scraping with a sterile pipette tip. For experiments examining biofilm establishment by one strain in

the presence of a mature biofilm developed by a different bacterial species, a single-species biofilm was grown for three days as describe above, prior to inoculation of the other species. The number of cultivable cells in the biofilms and in the biofilm supernatants was determined.

Quantification of cultivable cells

Bacterial suspensions were enumerated by counts of colony forming units (CFU). For this purpose, bacteria were serially 10-fold diluted, plated on LB-agar plates containing appropriate antibiotics, and grown for 16 h at 37°C. As previously described, in order to distinguish between the two bacterial species in the mixed cultures, LB-agar plates were supplemented with rifampicin (50 μg ml^{-1}) to recover Ec01 or ampicillin (30 μg ml^{-1}) to isolate Kp01 (Galván et al. 2016).

Growth inhibition assays

In order to explore a potential inhibitory activity toward Ec01 released by Kp01-containing biofilms, supernatants from seven-day-old single-species or mixed species biofilms were collected and filtered through a 0.22 μm pore size (Millipore, Bedford, MA, USA). For some assays, molecules present in the supernatants from mixed species biofilms were concentrated 10-fold by ultracentrifugation (3,000 MWCO Amicon Ultra, Millipore, Bedford, MA, USA). Ec01, pre-inoculated in LB, was suspended in the biofilm supernatants half-diluted with fresh AUM. For planktonic growth experiments, Ec01 (1×10^5 CFU ml^{-1}) was incubated at 37°C. Cultures were sampled at the indicated time points to determine the CFU ml^{-1} as described earlier. For biofilm growth assays, Ec01 (1×10^7 CFU ml^{-1}) was placed in 24-well culture plates as described above and incubated for 3 days at 37°C, replacing the half-diluted biofilm supernatant in each well every 24 h. At specified time points, planktonic cultures or disrupted biofilm suspensions were sampled to determine the number of cultivable cells.

Agar diffusion assay

To evaluate the antibacterial activity of biofilm supernatants against Ec01, LB- and AUM-agar plates (1.4% agar) containing Ec01 (10^6 CFU ml^{-1}) were prepared. Then, 20 μl of sample or appropriated control were loaded into holes pre-formed in the agar plate. After incubation for 16 h at 37°C, the appearance of a growth inhibition halo was monitored. Ampicillin and *Klebsiella pneumoniae* RYC492, a bacteriocin producing strain (de Lorenzo 1984), were used as positive controls for Ec01 growth inhibition.

Confocal laser scanning microscopy assay

Confocal laser scanning microscopy (CLSM) was used to visualize the different stages of biofilm formation on 22 mm-diameter siliconized coverslips. For this purpose, Ec01 carrying the tetracycline resistant plasmid pHC60, which expresses green fluorescent protein (GFPuv) (Cheng and Walker 1998), and Kp01 carrying the empty vector pHC60Δgfp were used. Biofilm formation was performed as described earlier (see Biofilm formation assay), using AUM supplemented with tetracycline (10 μg ml^{-1}). Briefly, sterile coverslips were placed inside six-well culture plates and inoculated with 4 ml of bacterial suspension (1×10^7 CFU ml^{-1}). The inoculated wells were incubated for 3 h at 37°C and then the medium was renewed every 24 h. At indicated time points, biofilms were rinsed with 0.9% NaCl and fixed in 4% paraformaldehyde in PBS for 2 h. Then, counterstaining with 130 μg ml^{-1} of propidium iodide (PI) for 1 h at room temperature was carried out. Coverslips were then mounted on a slide with a drop of mounting medium [90% glycerol in 100 mM NaH_2PO_4 and 10 mM Tris-HCl (pH 8)]. Observation of biofilms was done using a Carl Zeiss Pascal LSM 5-Axioplan 2 laser scanning confocal microscope (Zeiss, Oberkochen, Germany) with a C-Apochromat 40 × /1.2 W objective. Dual-color images were acquired by sequentially scanning with settings optimal for GFP (488-nm excitation with argon laser line and detection of emitted light between 505 and 530 nm) or PI (543-nm excitation with He/Ne laser line and detection of emitted light between 570 and 615 nm). Representative images (frames of 230 × 230 μm) were taken with an image resolution of 1,024 × 1,024 pixels. For each biofilm, at least four image-stacks were taken at different locations throughout the biofilm, using 1-μm *z*-step increments. Images were first analyzed by using the Zeiss LSM Image Browser version 3.2.0. Biofilm biomass and biofilm thickness (biofilm average height) were then quantified using the confocal *z*-stacks and images were analyzed using COMSTAT 2.1 (www.comstat.dk) (Heydorn et al. 2000; Vorregaard 2008) and ImageJ software (National Institutes of Health, MD, USA). In particular, time-course biomass progression of GFP-expressing Ec01 was determined for both single-species and mixed biofilms.

CAS assays

Siderophore production was evaluated by the chrome azurol S (CAS) agar assay described by Schwyn and Neilands (1987) and modified by Alexander and Zuberer (1991). The CAS dye (Sigma Aldrich, St Louis, MO, USA) can form stable complexes with ferric iron, resulting in a blue color when it is incorporated into the plates of

agarized medium. The medium turns orange to yellow when iron is removed from the CAS-Fe^{3+} complex by a chelator, such as a siderophore. Since casamino acids included in the medium formulation are a source of iron that could inhibit siderophore synthesis, 100 µM 2,2′-dipyridyl (DIP, Sigma Aldrich), a specific Fe^{2+} chelator, was added in order to achieve iron starvation and stimulate siderophore production. Strains were grown in 2 ml of AUM supplemented with 100 µM DIP for 48 h at 37°C. The planktonic cultures were standardized to 1×10^8 CFU ml^{-1} before 10 µl of each strain were spotted onto the CAS-Fe^{3+} agar plate with or without DIP supplementation. The plates were incubated at 37°C for 48 h and appearance of yellow/orange halos were monitored. *Pseudomonas aeruginosa* PA14 (Rahme et al. 1995) and *Acinetobacter baumannii* ATCC19606 (Garcia et al. 2012) strains were used as controls for siderophore production.

Bacterial growth in AUM supplemented with 2,2′-dipyridyl (DIP)

The ability of bacterial strains to grow in AUM depleted of Fe^{2+} (by supplementation with DIP) was examined. AUM-agar plates (1.5% agar) supplemented with 400 µM DIP alone, 400 µM DIP plus 10 µM $FeCl_3.6H_2O$ in 10 mM HCl (as a Fe^{3+} source), or without supplementation (for control of bacterial growth) were prepared. Strains were grown in 2 ml of AUM supplemented with 100 µM DIP for 48 h at 37°C. Then, bacterial cultures were standardized to 1×10^8 CFU ml^{-1} before 10 µl of each strain were spotted onto plates. The plates were then incubated at 37°C for 48 h and bacterial growth was visualized as colony formation on the plate and also quantified by CFU counts after disrupting the bacterial colonies in sterile 0.9% NaCl.

Statistical analysis

Statistical significance was assessed using one-way analysis of variance (ANOVA) with Bonferroni post-test. A p-value < 0.05 was considered significant. Analyses were performed using GraphPad Prism, version 4 (GraphPad Software, San Diego, CA, USA).

Results

Competitive interactions between K. pneumoniae *and* E. coli *in early-stage mixed biofilms developed on polystyrene*

Kp01-Ec01 mixed species biofilm development in AUM on a siliconized surface was previously investigated (Galván et al. 2016). These studies revealed that, despite the similar levels of initial adhesion to the surface of both bacterial species, a marked decline in the number of viable Ec01 cells was later found in mixed species biofilms. To analyze whether the surface material could influence this phenomena, biofilms were grown on polystyrene plates. When initial binding was measured after mixed inoculations, Kp01 showed approximately sevenfold higher adhesion to polystyrene than to silicone ($5.9 \pm 1.3 \times 10^5$ and $8.3 \pm 1.5 \times 10^4$ CFU cm^{-2}, respectively), whereas Ec01 binding to polystyrene was ~19-fold higher than to silicone ($1.6 \pm 0.7 \times 10^6$ and $8.6 \pm 4.4 \times 10^4$ CFU cm^{-2}, respectively). Similar results were observed for adhesion after single-species inoculations. Notably, despite the higher number of Ec01 cells initially bound to the polystyrene surface, compared to Kp01 (approximately threefold higher), Ec01 viability declined over time in mixed species biofilms until day 5 (Figure 1A). At this time point, the number of Ec01 cells was 1.6 logs lower in mixed *vs* single-species biofilm. This difference remained constant

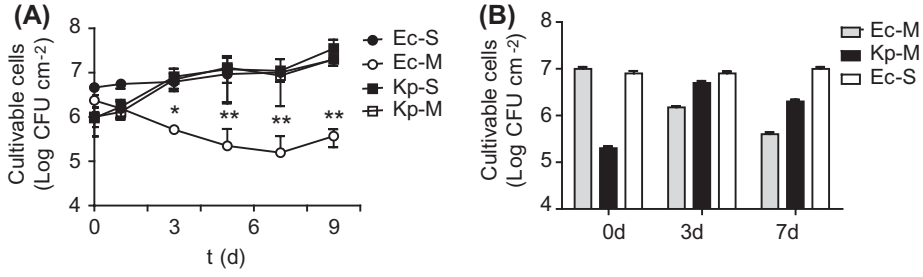

Figure 1. Bacterial behavior in *K. pneumoniae–E. coli* mixed biofilms compared to single-species biofilms. (A) Time-course of biofilm formation in AUM assessed as the number of cultivable cells cm^{-2} recovered from polystyrene plates. *E. coli* Ec01 and *K. pneumoniae* Kp01 strains from both single-species (Ec-S and Kp-S) and mixed (Ec-M and Kp-M) biofilms were studied. Each point represents the geometric mean ± SDs of at least three independent experiments. (*) $p < 0.01$ and (**) $p < 0.001$ for Ec01 in single-species *vs* mixed biofilms. (B) Effect on biofilm development of Kp01 colonization over a Ec01 pre-established biofilm. Ec01 single-species biofilm was grown for three days and then challenged with Kp01 (t=0). Cultivable cell numbers of Ec01 and Kp01 in mixed biofilms (Ec-M and Kp-M) were assessed at three and seven days after the Kp01 challenge as described in (A). Single-species Ec01 biofilm (Ec-S) was included as a control. Each bar represents the mean ± SE of two independent experiments.

at the latter stages of biofilm development (day 9 was the last time point assayed). In contrast, Kp01showed similar cell counts in single-species and mixed biofilms. These results also indicate that after a slightly lower initial adhesion of Kp01 compared to Ec01 (Kp01:Ec01 ratio, 1:2.7), at the early stages of biofilm development, a significant decrease in Ec01 viability, but not Kp01, occurred which is reflected in the Kp01:Ec01 ratio (55:1).

Next, Kp01 colonization of a mature Ec01 biofilm was examined to determine whether there was an effect on Ec01 viability. Figure 1B shows that Kp01 was able to colonize a three-day-old Ec01 biofilm. Moreover, the mixed species biofilm showed an increase in Kp01 cell numbers of ~21-fold and ~19-fold at days 3 and 7 post Kp01 challenge, respectively. Conversely, Ec01 viability decreased approximately sevenfold and ~25-fold at days 3 and 7 post Kp01 challenge, respectively. These results show that the detrimental effect of *K. pneumoniae* over *E. coli* can also occur after a mature *E. coli* biofilm had been developed.

To better understand these community dynamics and interbacterial interactions, time-course biofilm progression was monitored by CLMS, using an Ec01 strain carrying a plasmid that express GFP (Ec01-GFP) and visualizing Kp010 by counterstaining with propidium iodide after paraformaldehyde fixation. As shown by CFU counts, both bacterial species adhered well to the surface when inoculated alone or after co-inoculation (Figure 2A–C). Time-course determination of average biofilm thickness showed that both single- and dual-species biofilms increased their thickness over time in a similar fashion, reaching the greatest value at day 5 (Figure 2G). CFU counts at day 5 indicated no differences in Kp01 content were evident between single-species and mixed species biofilms (Figure 2E, F). However, there was a reduction of Ec01-GFP cells in mixed species biofilms compared to single-species biofilms (Figure 2D, F). Noticeably, Ec01-GFP cells were scattered along the predominant Kp01 biofilm (Figures 2F and S1). Quantification of Ec01-GFP biofilm biomass from the CLMS images indicated a significant reduction of Ec01-GFP biomass over time in mixed species biofilms with respect to single-species biofilms (Figure 2H). By day 5, a 60-fold reduction in Ec01-GFP biomass was observed in mixed species biofilms compared to single-species ones.

Supernatants of K. pneumoniae *biofilms exhibited neither antimicrobial nor anti-biofilm activities against* E. coli

To determine if the antagonistic effect of Kp01 on Ec01 populations in mixed species biofilms was the result of a secreted effector with antimicrobial activity, Kp01 supernatants from seven-day-old single-species or mixed species biofilms were tested for their antimicrobial effect on Ec01. First, supernatants were tested by the agar diffusion method on Ec01 growing either on LB- or AUM-agar plates (Figure 3A and B). As expected, better bacterial growth was achieved in the rich medium, LB, than in the minimal medium, AUM. Regarding supernatant antimicrobial activities, neither Kp01 nor mixed species biofilm supernatants showed inhibitory effects of Ec01 growth. Moreover, a 10-fold concentrated supernatant from mixed species biofilms showed similar results (data not shown). In contrast, ampicillin and the microcin-producing *K. pneumoniae* RYC492 (de Lorenzo 1984) were able to inhibit Ec01 growth in both the media tested or only in LB, respectively. In addition, Ec01 planktonic growth kinetics were tested in supernatants supplemented 1:1 (v v^{-1}) with fresh AUM. Neither supernatants from Kp01 biofilms nor supernatants from mixed species biofilms significantly affected Ec01 growth (Figure 3C). Moreover, a 10-fold concentrated supernatant from mixed species biofilms showed similar results. Finally, the ability of Ec01 to establish a biofilm in the presence of supernatants from mixed or single-species Kp01 biofilms was tested. Biofilms grown for three days in supernatants supplemented 1:1 (v v^{-1}) with fresh AUM showed fivefold fewer viable bacteria compared to the control biofilms developed in AUM (Figure 3D). However, this decrease was not only observed in the presence of Kp01 single-species and mixed species supernatants, but also when Ec01 supernatants were tested. These results did not indicate the presence of a secreted effector with antimicrobial activity against *E. coli* or with anti-biofilm activity from *K. pneumoniae* single or mixed species biofilms.

Continuous nutrient delivery abolished the competitive effect of K. pneumoniae *over* E. coli *in mixed biofilms*

In order to investigate whether nutritional competition is involved in the detrimental effect of Kp01 over Ec01, biofilms formed under continuous nutrient supply (37 ml h^{-1}) were compared to batch-fed biofilms, at three days after bacterial inoculation. All continuous-flow biofilms exhibited fivefold higher cell numbers than the corresponding batch-fed biofilms (Figure 4A and B). This result indicate that a continuous influx of fresh medium allows better growth of both bacterial species. Contrary to the expected decrease in Ec01 cells in batch-fed mixed species biofilms, similar levels of Ec01 cells were observed in mixed continuous-flow biofilms, compared to single-species ones. Moreover, when dispersed cells from biofilms were quantified, a similar behavior was found (Figure 4C and D). These results suggest that nutrient limitation is involved

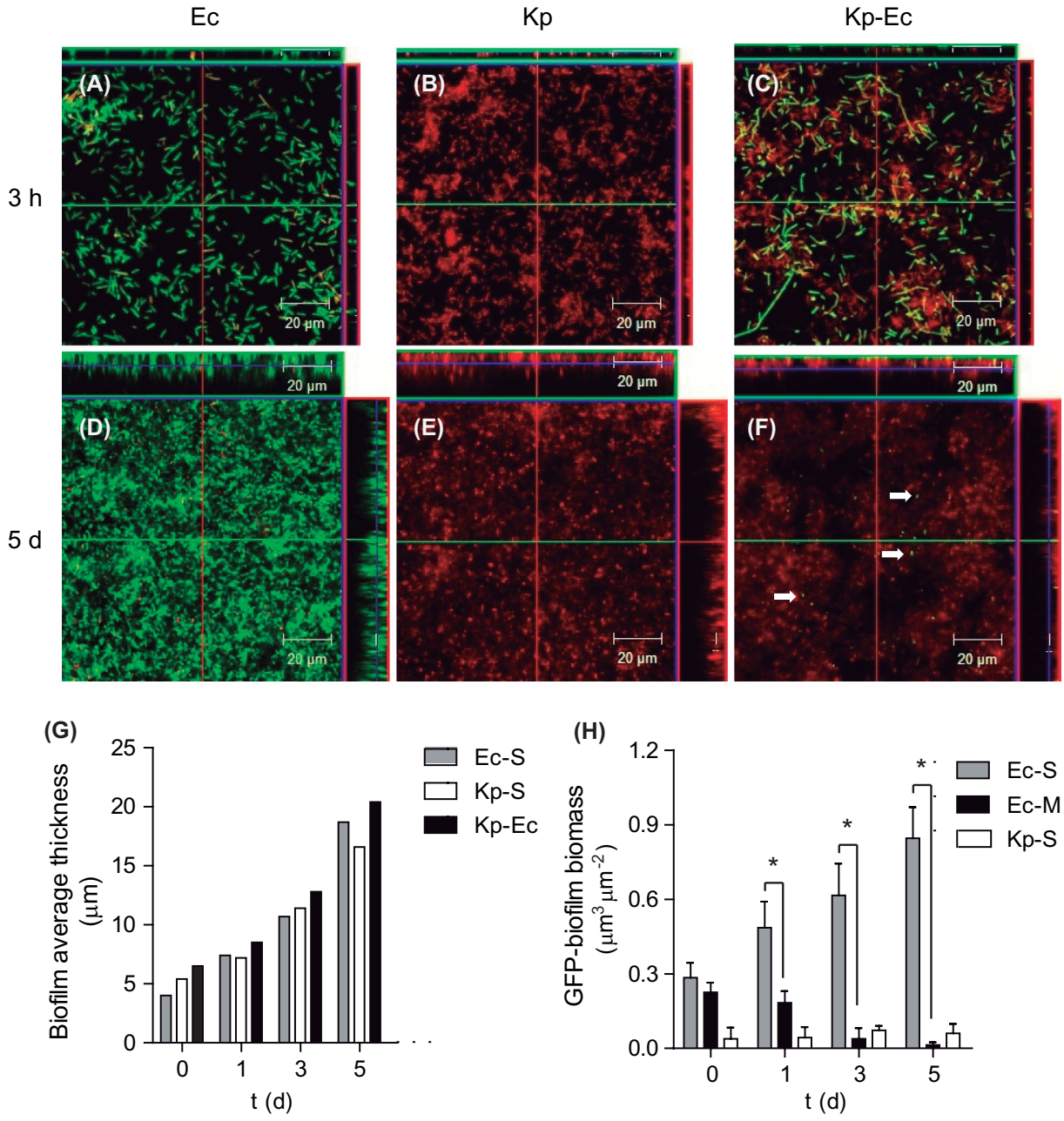

Figure 2. Confocal scanning laser microscopy of *E. coli* Ec01 single-species (Ec), *K. pneumoniae* Kp01 (Kp) single-species, and mixed (Kp-Ec) biofilms. Representative images taken at the surface level after initial adhesion of the cells (3 h) (A–C) or taken at 5 µm above the surface for five-day-old biofilms (D–F). Green indicates GFP fluorescence and the presence of Ec01; red indicates propidium iodide, which stains nucleic acids of either bacterial species. Magnification, × 400; scale bars represent 20 µm. White arrows indicate scattered Ec01 GFP (green–yellow) along the predominant Kp01 biofilm (red). (G) Biofilm average thickness and (H) *E. coli* (GFP) biomass quantification of biofilms. At least four z-stacks of each time point were analyzed using COMSTAT software. (*) $p < 0.001$ for *E. coli* in single *vs* mixed biofilms, at indicated times.

in the outcompeting mechanism of *K. pneumoniae* over *E. coli*.

Iron scavenging ability of K. pneumoniae *and* E. coli

Iron is an essential element required by microorganisms to grow (Barber and Elde 2015). The production of iron-scavenging molecules called siderophores was screened initially by the universal CAS agar assay. In CAS agar plates, both Kp01 and Ec01 were moderately positive, showing a yellowish halo around the bacterial colony (1.2 and 1.1 cm, respectively) (Figure 5A). Regarding the control strains, *P. aeruginosa* produced a small yellowish halo (0.7 cm), whereas *A. baumanii* showed a 1.1 cm halo. In

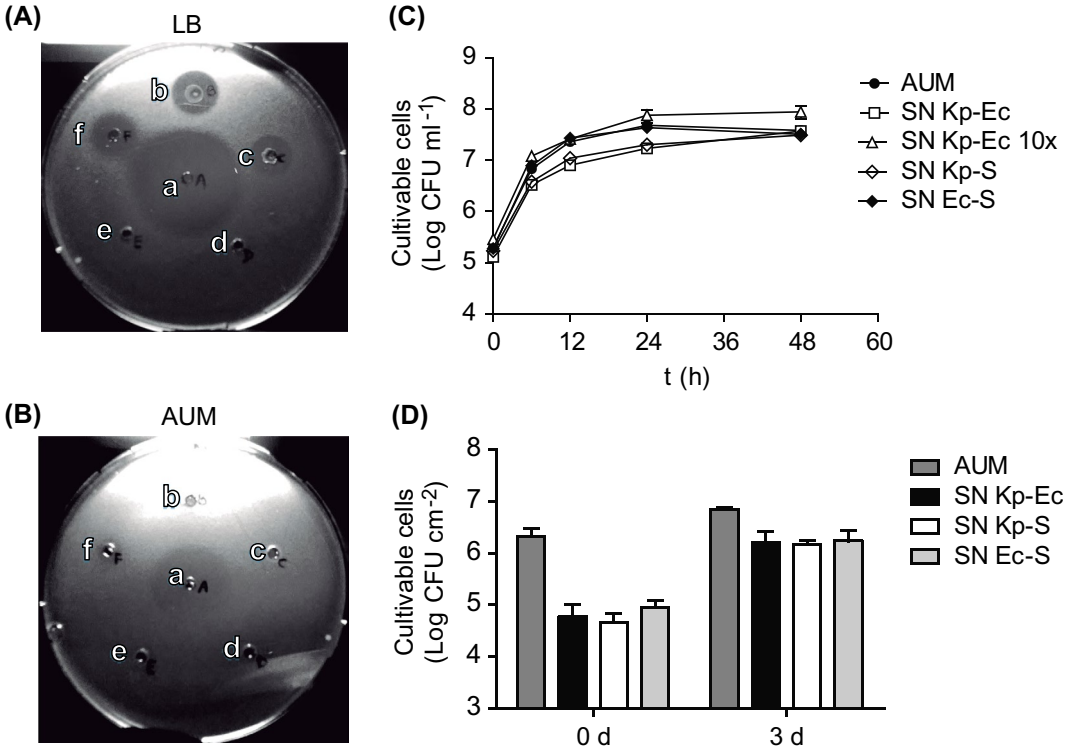

Figure 3. *E. coli* growth in the presence of biofilm supernatants. Cell-free supernatants (SN) from seven-day-old single-species and mixed biofilms were analyzed. (A and B) Agar well diffusion assays using Ec01 as the test organism, growing in LB-agar (A) or AUM-agar (B) plates. Compounds tested: (a) Ap (60 μg ml^{-1}); (b) microcin-producing strain Kp RYC492 (10^7 CFU ml^{-1}); (c) SN from overnight liquid culture of Kp RYC492; (d) SN from Kp01 biofilm; (e) SN from mixed biofilm; (f) Ap (6 μg ml^{-1}). (C) Time-course of Ec01 planktonic growth in AUM containing biofilm SN at a ratio 1:1. SN mix 10× indicates that a 10-fold concentrated biofilm was assayed. The number of cultivable cells ml^{-1} was determined as described in Materials and methods. Each point represents the mean of two independent experiments, with <10% difference in the values obtained in each assay. (D) Ec01 biofilms developed in the presence of biofilm SNs. Biofilm SNs were added from the beginning of the assay. Cultivable cells cm^{-2} recovered from three-day-old biofilms are shown. Each bar represents the mean ± SE of two independent experiments.

order to achieve iron starvation and stimulate siderophore production, the specific Fe^{2+} chelator 2,2′dipiridyl (DIP) was added to the CAS agar plates (Figure 5B). Addition of DIP clearly stimulated siderophore production of all strains, as reflected by the size increase of the yellow halos. The effect was greater on Kp01, with a substantial increase in the halo size compared to Ec01 (2.7 *vs* 1.2 cm, respectively). These results suggest that under iron limitation *K. pneumoniae* has a more effective siderophore production response. Then, the ability of each bacterial species to grow in AUM-agar plates supplemented with increased concentrations of DIP was assayed. DIP concentrations up to 200 μM did not significantly affect Kp01 nor Ec01 growth in AUM (Figure S2). However, addition of 400 μM DIP to AUM-agar plates strongly inhibited bacterial growth [$(24 \pm 4) \times 10^7$ *vs* $(0.7 \pm 0.2) \times 10^7$ cells per bacterial spot and $(12 \pm 2) \times 10^7$ *vs* $(0.03 \pm 0.02) \times 10^7$ cells per bacterial spot for *K. pneumoniae* and *E. coli*, respectively, in AUM *vs* AUM plus DIP], (Figure 5D). Additional supplementation with Fe^{3+} partially reverted the Kp01 growth inhibition, evidencing the ability of *K. pneumoniae* to utilize ferric iron probably by siderophore(s) production (Figure 5E). Conversely, even after Fe^{3+} supplementation *E. coli* was not able to restore its growth.

These results suggest that *K. pneumoniae* is more efficient than *E. coli* in growing in environments with limited iron availability. This could be the situation in mixed species biofilms developed in AUM.

Discussion

Microbial biofilms are an increasing concern in the medical field where the use of artificial medical devices for therapeutic and restorative purposes is on the rise. Biofilms are frequently found as multispecies communities that differ greatly in composition, structure, and antimicrobial resistance from mono-species biofilm systems (Liu et al. 2016). The catheterized urinary tract provides ideal conditions for the development of biofilm populations (Chenoweth et al. 2014). In this investigation, the

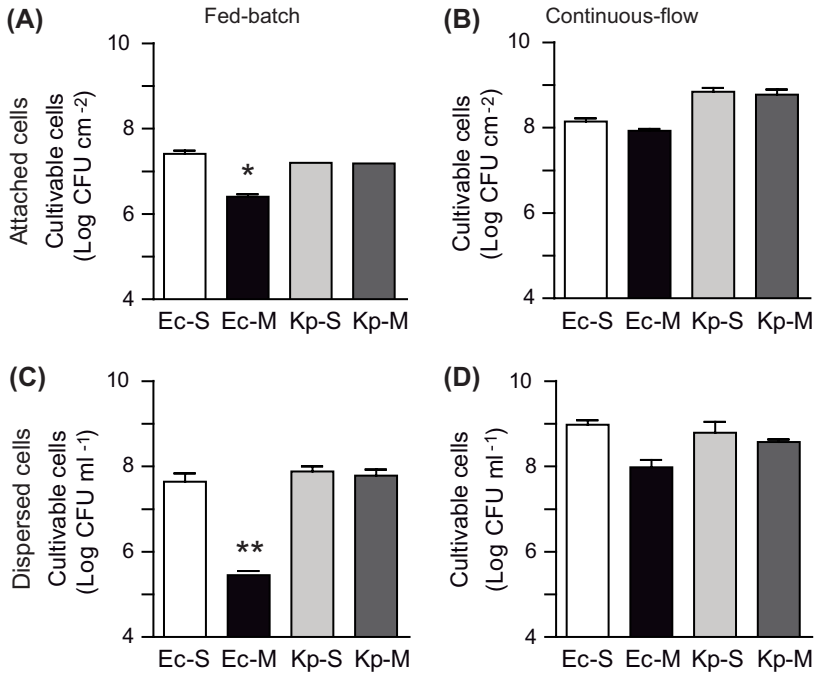

Figure 4. Comparison of bacterial coexistence in static *vs* dynamic biofilms. Biofilms were developed in batch culture (with AUM change every 24 h) (panels A and C) or under continuous AUM flow (37 ml min^{-1}) (panels B and D). The number of cultivable cells obtained from attached bacteria forming biofilms (panels A and B) and from bacteria in the medium surrounding the biofilms (panels C and D) were assessed as described in the Materials and methods section. Single-species and mixed biofilms were analyzed. Each bar represents the mean ± SD of three independent experiments. (*) $p < 0.05$ and (**) $p < 0.01$ for *E. coli* in single-species *vs* mixed biofilms.

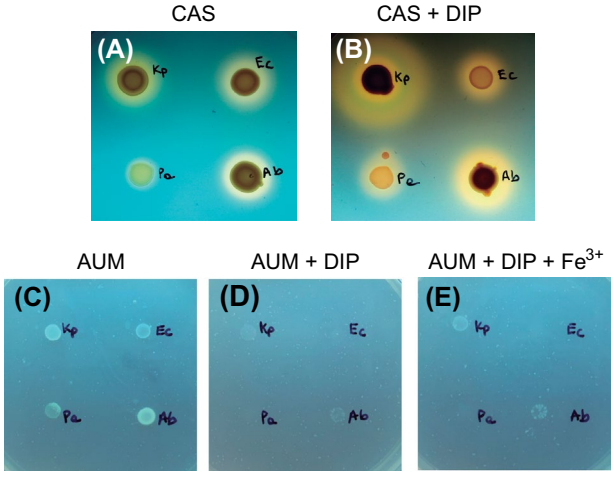

Figure 5. Production of siderophores screened by the CAS agar assay (A, B) and the effect of iron availability on bacterial growth on AUM agar plates (C–E). Bacterial strains assayed: *K. pneumoniae* Kp01 (Kp), *E. coli* Ec01 (Ec), *P. aeruginosa* PA14 (Pa), and *A. baumanii* ATCC 19,606 (Ab). (A, B) CAS agar plates without (A) or with 100 µM DIP (B). Note the appearance of yellow halos around the colonies, indicating siderophore production. (C–E) Bacterial growth on AUM agar plates without supplementation (C), supplemented with (D) 400 µM DIP or (E) 400 µM DIP plus 10 µM $FeCl_3$. In all cases, one representative assay, from two independent experiments, is shown.

authors focused on understanding a *K. pneumoniae* and *E. coli* mixed biofilm, as the two species can coexist during CAUTIs (Galván et al. 2016) (Ganderton et al. 1992; Wang et al. 2010). CAUTIs are frequently recalcitrant to existing antimicrobial treatments; therefore, established biofilms are not eradicated completely after treatment and surviving biofilm cells could carry on the infection. Additionally, even though in a patient with CAUTI, the catheter can be removed to eliminate the source of biofilm itself while the patient is treated with antibiotics to kill planktonic bacteria, uropathogens such as *E. coli* and *K. pneumoniae* are able to survive in the host by invading the bladder epithelium (Flores-Mireles et al. 2015). Invasion allows the bacteria to subvert host defenses and become recalcitrant to antibiotic treatments by forming transient biofilm-like intracellular bacterial communities and quiescent intracellular reservoirs. Bacteria can disperse from these structures and then invade other cells or colonize a newly applied catheter. Moreover, *K. pneumoniae* and *E. coli* are both highly antibiotic-resistant organisms (WHO 2014). These facts highlight the importance of understanding the underlying mechanisms of interspecies interaction between these two species in biofilms, which could help to identify potential

targets for therapeutic intervention. Although *K. pneumoniae–E. coli* mixed species biofilms formed in AUM have previously been studied, the interactions between these two species have yet to be fully characterized. As previously reported, after co-inoculation at a 1:1 ratio, both bacterial species adhered at similar levels to both siliconized and polystyrene surfaces; however, at early-stages of biofilm development (less than three days) *K. pneumoniae* outcompeted *E. coli* (Galván et al. 2016). Here, prolonged (more than five days) batch-fed biofilm growth showed that both bacteria coexist in mixed species biofilms at a *K. pneumoniae*:*E. coli* ratio of ~55:1. In fact, *K. pneumoniae* showed similar cell counts in single-species and mixed species biofilms, which was in agreement with the findings reported previously, in which mixed species biofilms were formed on a siliconized surface (Galván et al. 2016). Based on these results, it was concluded that *K. pneumoniae* partially outcompeted *E. coli* in early stages of mixed biofilms, whereas in later stages (after day 5) both bacterial species coexisted. A similar competitive effect was observed after the addition of *K. pneumoniae* to a pre-established *E. coli* biofilm. Moreover, even when *E. coli* was able to adhere to a pre-formed *K. pneumoniae* biofilm (3×10^6 cells cm^{-2}), an ~2-log decrease in *E. coli* cell number was observed after three days of mixed species biofilm development with no additional loss in *E. coli* viability subsequently observed (data not shown). The analysis of spatial organization of the mixed species biofilm by CLSM corresponded to the results obtained by CFU counts. At 3 h, both species were found well adhered on the surface. However, at later times it was possible to visualize *K. pneumoniae* outcompeting *E. coli*. It has been postulated that bacterial species organize in three general forms: interspecific segregation, coaggregation, and/or stratification, based on different types of interspecies interactions (Liu et al. 2016). For adhesion to the surface, *K. pneumoniae* and *E. coli* in mixed biofilms might be following a co-aggregation pattern, with both species being well intermixed on the surface. Unfortunately, CLSM images did not give enough information to form conclusions regarding bacterial co-aggregation and further tests will need to be conducted. At extended times, no segregation or stratification was detected. By the time a clear displacement of *E. coli* occurred, the remaining *E. coli* detected in the mixed species biofilm were found scattered among the predominant *K. pneumoniae* cells.

Mechanisms of biofilm competition have been classified in two groups: 'interference competition', that refers to specific mechanisms which damage a competitor's survival, and 'exploitative competition', which corresponds to indirect interactions by which one organism prevents access to and/or limits the use of resources by another organism (Rendueles and Ghigo 2015). Analysis of antimicrobial activity of mixed species biofilm supernatants on *E. coli* growing either in solid medium or in broth failed to detect secreted antimicrobial compounds. It could be that antimicrobial compounds are present at very low concentrations, which would also appear as a negative result. However, even when a 10-fold concentrated supernatant from mixed species biofilms was tested, no antimicrobial activity was detected. These results suggest that the decrease in *E. coli* cells when forming a mixed species biofilm with *K. pneumoniae* is probably not due to the production of antimicrobial compounds by *K. pneumoniae*. Additionally, biofilm supernatants did not exhibit anti-biofilm activity against *E. coli*, as shown by a similar performance of *E. coli* biofilm development in the presence of supernatants from *K. pneumoniae* and *E. coli* single-species biofilm as well as supernatants from mixed species biofilms. Even though initial adhesion of *E. coli* was less in the presence of biofilm supernatants than in AUM, since this effect was observed for all supernatants including the supernatants from single-species *E. coli* biofilms, it could be possible that this is due to the increase in the pH of these samples compared to fresh AUM (7.8 *vs* 6.8, respectively). Whereas the rising pH in supernatants from *K. pneumoniae* containing biofilms could be due to the expression of *K. pneumoniae* urease (which is able to generate NH_3 by urea cleavage), the reason for pH alcalinization in supernatants from single-species *E. coli* biofilms is still unclear.

Since bacterial growth is dependent on the concentration of limiting resources (eg iron, carbon and oxygen) in the biofilm environment, the availability of such resources could drive competition (Rendueles and Ghigo 2015). In particular, AUM is a minimal medium that mimics human urine composition (Brooks and Keevil 1997). To analyze this possibility, bacterial cell numbers were assessed in mixed biofilms formed under a continuous nutrient supply. Under a continuous influx of AUM, the numbers of biofilm-associated *E. coli* and *K. pneumoniae* were not affected by the presence of the other species. Comparison of this result with that obtained in batch-fed biofilm experiments supports the idea that an exploitative competition of *K. pneumoniae* over *E. coli* in mixed species biofilms could be driven by nutrient limitation. Exploitation of a variety of essential elements, including oxygen, carbon, phosphorous, and especially iron have been reported (Rendueles and Ghigo 2015). Iron is a key element in microbial physiology, controlling many bacterial functions. Due to its low bioavailability, bacteria have evolved many iron-scavenging strategies, such as high-affinity iron-chelators or siderophores. Siderophore-producing genotypes increase their own growth rate while they deplete iron in their surroundings and potentially

limit access to it for other genotypes (Eberl and Collinson 2009; Barber and Elde 2015). The repertoire of siderophores varies among different microbial species and even among different strains. Indeed, various combinations of siderophores (eg aerobactin, enterobactin, salmochelin and yersiniabactin) are found among clinical isolates of *Klebsiella pneumoniae* and *E. coli* (Henderson et al. 2009; El Fertas-Aissani et al. 2013). In this regard, siderophore production of the two species under study were analyzed by the CAS assay. *K. pneumoniae* produced a noticeable yellow halo, indicative of siderophore production, that increased in size when the Fe^{2+} chelator DIP was added to the plate. Conversely, whereas *E. coli* showed a yellowish halo in CAS plates, this halo did not significantly increase in the presence of DIP. These results suggest that *K. pneumoniae* is able to express high amounts of siderophore molecules in response to iron starvation, whereas *E. coli* does that to a much lesser extent. Moreover, assays performed in AUM-agar plates in the presence of a high DIP concentration (400 μM), to evaluate growing capacity under a pronounced iron starvation in AUM, evidenced a better ability of *K. pneumoniae* to grow in this condition than *E. coli*. Furthermore, addition of Fe^{3+} together with DIP to the AUM agar plates improved *K. pneumoniae*, but not *E. coli*, growth. This result suggests that *K. pneumoniae* has a better ability than *E. coli* to utilize ferric iron, probably due to more efficient siderophore production. Additional ongoing research efforts are focused on identifying the siderophores expressed by both bacterial species when growing together in mixed biofilms developed in AUM. It is important to note that the iron levels present in the AUM used in the present culture experiments (250 ± 40 μg l^{-1} are similar to the reported iron concentrations observed in human urine, which can vary from 152 to 419 μg l^{-1} depending on the age of the individual, with higher levels being found in older people (Pfrimer et al. 2014). Interestingly, urine is a complex and variable biofluid whose chemical composition is shaped by multiple sources, including the host metabolism and the intestinal microbiome (Bouatra et al. 2013). Therefore, variations in free iron levels originated from individual differences in urine composition may add more complexity to the modulation of siderophore expression by both *K. pneumoniae* and *E. coli*. In particular, patients with inflammatory damage of the tissue, traumatism, or other disorders such as hemochromatosis, could generate an environment with high iron availability; consequently, nutritional competition between *K. pneumonia* and *E. coli* strains for available iron might be impaired and a polymicrobial infection could be facilitated.

Altogether, the results presented here showed the killing of some of the original *E. coli* adhered cells at early stages of mixed *K. pneumoniae–E. coli* biofilm development; nevertheless, a fairly stable coexistence occurred in the long term. This long-term mixed biofilm contained ~55-fold more *K. pneumoniae* cells than *E. coli* cells. Evidence reported in this study pointed to iron utilization as a competing mechanism. However, a recent study has reported an alternative competitive mechanism in *K. pneumoniae*, in which *E. coli* could be susceptible to the expression of a type six secretion system (T6SS) (Liu et al. 2017). It cannot be ruled out that the competitive effect observed at early-stage mixed species biofilm formation involves the transient expression of this kind of secretion system. Overall, the data presented here may add to the understanding of the complex relationships between bacterial species in the context of polymicrobial biofilms formed on urinary catheters. From a clinical point of view, it seems that strategies tending to reduce the nutritional quality of urine in catheterized patients would be important to hinder catheter colonization and biofilm persistence by uropathogens. Particularly, to minimize iron availability in urine could be important in inhibiting bacterial growth in the urinary tract. Finally, elucidation of the mechanisms mediating interspecies interactions of two highly antibiotic resistant uropathogens such as *K. pneumoniae* and *E. coli*, which are prevalent pathogens in CAUTIs, may provide insight into new strategies for treatment of patients suffering from polymicrobial CAUTIs.

Acknowledgments

The authors are grateful to Claudia Garbasz, Head of the Microbiology Service at the Hospital General de Agudos "Dr I. Pirovano" (Buenos Aires city, Argentina) and Dr Beatriz Passerini de Rossi from Facultad de Farmacia y Bioquimica at the Universidad de Buenos Aires (Buenos Aires city, Argentina) for providing the bacterial isolates. They also thank Dr Walter Draghi from the Instituto de Biotecnología y Biología Molecular (La Plata, Buenos Aires, Argentina) and members of the laboratory of Dr Angeles Zorreguieta at Fundacion Instituto Leloir (Buenos Aires city, Argentina) for helping with the CAS assay. The authors also acknowledge the Servicio de Microscopia at Fundación Instituto Leloir (Buenos Aires city), for helping with the confocal microscopy. G.E.J. is a postdoctoral fellow and E.M.G. is a Career Investigator for CONICET.

Disclosure statement

No potential conflict of interest was reported by the authors.

Funding

This work was financially supported by the National Research Council of Argentina (CONICET) [grant number PIP 11220130100426CO] and intramural funding from the University of Maimonides, CEBBAD Center, Buenos Aires city, Argentina.

References

Alexander DB, Zuberer DA. 1991. Use of chrome azurol S reagents to evaluate siderophore production by rhizosphere bacteria. Biol Fertil Soils. 12:39–45. doi:10.1007/BF00369386

Alteri, CJ, Mobley, HL 2015. Metabolism and fitness of urinary tract pathogens. Microbiol Spectr 3. doi:10.1128/microbiolspec.MBP-0016-2015

Alteri CJ, Himpsl SD, Mobley HL. 2015. Preferential use of central metabolism *in vivo* reveals a nutritional basis for polymicrobial infection. PLoS Pathog. 11:e1004601. doi:10.1371/journal.ppat.1004601

Azevedo AS, Almeida C, Melo LF, Azevedo NF. 2014. Interaction between atypical microorganisms and *E. coli* in catheter-associated urinary tract biofilms. Biofouling. 30:893–902. doi:10.1080/08927014.2014.944173

Barber MF, Elde NC. 2015. Buried treasure: evolutionary perspectives on microbial iron piracy. Trends Genet. 31:627–636. doi:10.1016/j.tig.2015.09.001

Bouatra S, Aziat F, Mandal R, Guo AC, Wilson MR, Knox C, Bjorndahl TC, Krishnamurthy R, Saleem F, Liu P, et al. 2013. The human urine metabolome. PLoS ONE. 8:e73076. doi:10.1371/journal.pone.0073076

Brooks T, Keevil CW. 1997. A simple artificial urine for the growth of urinary pathogens. Lett Appl Microbiol. 24:203–206. doi:10.1046/j.1472-765X.1997.00378.x

Burmolle M, Webb JS, Rao D, Hansen LH, Sorensen SJ, Kjelleberg S. 2006. Enhanced biofilm formation and increased resistance to antimicrobial agents and bacterial invasion are caused by synergistic interactions in multispecies biofilms. Appl Environ Microbiol. 72:3916–3923. doi: 10.1128/AEM.03022-05

Cerqueira L, Oliveira JA, Nicolau A, Azevedo NF, Vieira MJ. 2013. Biofilm formation with mixed cultures of *Pseudomonas aeruginosa/Escherichia coli* on silicone using artificial urine to mimic urinary catheters. Biofouling. 29:829–840. doi:10.1080/08927014.2013.807913

Cheng HP, Walker GC. 1998. Succinoglycan is required for initiation and elongation of infection threads during nodulation of alfalfa by *Rhizobium meliloti*. J Bacteriol. 180:5183–5191.

Chenoweth CE, Gould CV, Saint S. 2014. Diagnosis, management, and prevention of catheter-associated urinary tract infections. Infect Dis Clin North Am. 28:105–119. doi:10.1016/j.idc.2013.09.002

Eberl HJ, Collinson S. 2009. A modeling and simulation study of siderophore mediated antagonism in dual-species biofilms. Theor Biol Med Model. 6:30. doi: 10.1186/1742-4682-6-30. doi:10.1186/1742-4682-6-30

El Fertas-Aissani R, Messai Y, Alouache S, Bakour R. 2013. Virulence profiles and antibiotic susceptibility patterns of *Klebsiella pneumoniae* strains isolated from different clinical specimens. Pathol Biol (Paris). 61:209–216. doi:10.1016/j.patbio.2012.10.004

Flemming HC, Wingender J, Szewzyk U, Steinberg P, Rice SA, Kjelleberg S. 2016. Biofilms: an emergent form of bacterial life. Nat Rev Microbiol. 14:563–575. doi:10.1038/nrmicro.2016.94

Flores-Mireles AL, Walker JN, Caparon M, Hultgren SJ. 2015. Urinary tract infections: epidemiology, mechanisms of infection and treatment options. Nat Rev Microbiol. 13:269–284. doi:10.1038/nrmicro3432

Foxman B. 2014. Urinary tract infection syndromes: occurrence, recurrence, bacteriology, risk factors, and disease burden. Infect Dis Clin North Am. 28:1–13. doi:10.1016/j.idc.2013.09.003

Galván EM, Mateyca C, Ielpi L. 2016. Role of interspecies interactions in dual-species biofilms developed *in vitro* by uropathogens isolated from polymicrobial urinary catheter-associated bacteriuria. Biofouling. 32:1067–1077. doi:10.1080/08927014.2016.1231300

Ganderton L, Chawla J, Winters C, Wimpenny J, Stickler D. 1992. Scanning electron microscopy of bacterial biofilms on indwelling bladder catheters. Eur J Clin Microbiol Infect Dis. 11:789–796. doi:10.1007/BF01960877

Garcia CA, Passerini De Rossi B, Alcaraz E, Vay C, Franco M. 2012. Siderophores of *Stenotrophomonas maltophilia*: detection and determination of their chemical nature. Rev Argent Microbiol. 44:150–154.

Hall-Stoodley L, Costerton JW, Stoodley P. 2004. Bacterial biofilms: from the natural environment to infectious diseases. Nat Rev Microbiol. 2:95–108. doi:10.1038/nrmicro821

Hancock V, Ferrieres L, Klemm P. 2008. The ferric yersiniabactin uptake receptor FyuA is required for efficient biofilm formation by urinary tract infectious *Escherichia coli* in human urine. Microbiology. 154:167–175. doi:10.1099/mic.0.2007/011981-0

Harriott MM, Noverr MC. 2009. *Candida albicans and Staphylococcus aureus* form polymicrobial biofilms: effects on antimicrobial resistance. Antimicrob Agents Chemother. 53:3914–3922. doi:10.1128/AAC.00657-09

Henderson JP, Crowley JR, Pinkner JS, Walker JN, Tsukayama P, Stamm WE, Hooton TM, Hultgren SJ. 2009. Quantitative metabolomics reveals an epigenetic blueprint for iron acquisition in uropathogenic *Escherichia coli*. PLoS Pathog. 5:e1000305. doi:10.1371/journal.ppat.1000305

Heydorn A, Nielsen AT, Hentzer M, Sternberg C, Givskov M, Ersbøll BK, Molin S. 2000. Quantification of biofilm structures by the novel computer program comstat. Microbiology. 146:2395–2407. doi:10.1099/00221287-146-10-2395

Holá V, Ruzicka F, Horka M. 2010. Microbial diversity in biofilm infections of the urinary tract with the use of sonication techniques. FEMS Immunol Med Microbiol. 59:525–528. doi:10.1111/j.1574-695X.2010.00703.x

Liu W, Roder HL, Madsen JS, Bjarnsholt T, Sorensen SJ, Burmolle M. 2016. Interspecific bacterial interactions are reflected in multispecies biofilm spatial organization. Front Microbiol. 7:1366.

Liu L, Ye M, Li X, Li J, Deng Z, Yao YF, Ou HY. 2017. Identification and characterization of an antibacterial type VI secretion system in the carbapenem-resistant strain *Klebsiella pneumoniae* HS11286. Front Cell Infect Microbiol. 7:15. doi:10.3389/fcimb.2017.00442

de Lorenzo V. 1984. Isolation and characterization of microcin E492 from *Klebsiella pneumoniae*. Arch Microbiol. 139:72–75. doi:10.1007/BF00692715

Moreno E, Andreu A, Pérez T, Sabaté M, Johnson JR, Prats G. 2006. Relationship between *Escherichia coli* strains causing urinary tract infection in women and the dominant faecal flora of the same hosts. Epidemiol Infect. 134:1015–1023. doi:10.1017/S0950268806005917

Pfrimer K, Micheletto RF, Marchini JS, Padovan GJ, Moriguti JC, Ferriolli E. 2014. Impact of aging on urinary excretion of iron and zinc. Nutr Metab Insights. 7:47–50. doi:10.4137/NMI.S12977

Rahme LG, Stevens EJ, Wolfort SF, Shao J, Tompkins RG, Ausubel FM. 1995. Common virulence factors for bacterial pathogenicity in plants and animals. Science. 268:1899–1902. doi:10.1126/science.7604262

Reisner A, Maierl M, Jorger M, Krause R, Berger D, Haid A, Tesic D, Zechner EL. 2014. Type 1 fimbriae contribute to catheter-associated urinary tract infections caused by *Escherichia coli*. J Bacteriol. 196:931–939. doi:10.1128/JB.00985-13

Rendueles, O, Ghigo, JM. 2015. Mechanisms of competition in biofilm communities. Microbiol Spectr 3. doi:10.1128/microbiolspec.MB-0009-2014

Sabir, N, Ikram, A, Zaman, G, Satti, L, Gardezi A, Ahmed A, Ahmed P 2017. Bacterial biofilm-based catheter-associated urinary tract infections: causative pathogens and antibiotic resistance. Am J Infect Control. 45:1101–1105. doi:10.1016/j.ajic.2017.05.009

Schroll C, Barken KB, Krogfelt KA, Struve C. 2010. Role of type 1 and type 3 fimbriae in *Klebsiella pneumoniae* biofilm formation. BMC Microbiol. 10:179. doi:10.1186/1471-2180-10-179

Schwyn B, Neilands JB. 1987. Universal chemical assay for the detection and determination of siderophores. Anal Biochem. 160:47–56. doi:10.1016/0003-2697(87)90612-9

Stickler DJ. 2008. Bacterial biofilms in patients with indwelling urinary catheters. Nat Clin Pract Urol. 5:598–608. doi:10.1038/ncpuro1231

Stickler DJ, Morgan SD. 2006. Modulation of crystalline *Proteus mirabilis* biofilm development on urinary catheters. J Med Microbiol. 55:489–494. doi:10.1099/jmm.0.46404-0

Subashchandrabose S, Mobley HL. 2015. Back to the metal age: battle for metals at the host-pathogen interface during urinary tract infection. Metallomics. 7:935–942. doi:10.1039/C4MT00329B

Tan CH, Lee KW, Burmølle M, Kjelleberg S, Rice SA. 2017. All together now: experimental multispecies biofilm model systems. Environ Microbiol. 19:42–53. doi:10.1111/1462-2920.13594

Vorregaard M. 2008. Comstat2 - a modern 3D image analysis environment for biofilms, in informatics and mathematical modelling. Kongens Lyngby, Denmark: Technical University of Denmark.

Wang X, Lünsdorf H, Ehrén I, Brauner A, Römling U. 2010. Characteristics of biofilms from urinary tract catheters and presence of biofilm-related components in *Escherichia coli*. Curr Microbiol. 60:446–453. doi:10.1007/s00284-009-9563-z

Warren JW, Tenney JH, Hoopes JM, Muncie HL, Anthony WC. 1982. A prospective microbiologic study of bacteriuria in patients with chronic indwelling urethral catheters. J Infect Dis. 146:719–723. doi:10.1093/infdis/146.6.719

WHO. 2014. Antimicrobial resistance global report on surveillance. Geneva: World Health Organization, 256 pp.